

# Energy Harvesting Simulation of Piezoelectric ZnO for Electromechanical Nanogenerators

Wen-Yang Chang<sup>1\*</sup>, Cheng-Han Yang<sup>2</sup>

<sup>1</sup>Assistant Professor, Department of Mechanical and Computer-Aided Engineering, National Formosa University  
64 Wunhua Rd., Huwei Township, Yunlin County 632, Taiwan

<sup>2</sup>Graduate student, Department of Mechanical and Computer-Aided Engineering, National Formosa University  
64 Wunhua Rd., Huwei Township, Yunlin County 632, Taiwan

\*wenyang@nfu.edu.tw

## Abstract

The study investigates the piezoelectric harvesting efficiency of ZnO microstructures with various structural configurations for electromechanical nanogenerators using finite element method simulation. The effects of ZnO structural parameters for a given cross-section area are simulated, including length, height, array number and shape. In addition, the harmonic responses and model frequencies are evaluated to analyze the natural mode shapes and force vibrations.

The results show that the energy harvesting efficiency increases with decreasing ratio ( $R_h$ ) of the diameter to the height. However, the trend of the harvesting voltage becomes almost saturated when the  $R_h$  ratio is less than 0.5. A single bulk structure of piezoelectric ZnO produces less micro-energy than that produced by an array structure for given cross-section area. The harvesting voltage increases with increasing number of arrays. The conversion efficiencies of 6, 11, 19 and 22 arrays increases 93.4, 187.3, 345.6 and 537.2 %, respectively, that are compared to the single-bulk output powers. However, the energy harvesting efficiency decreases when the array number is over 33 for arrays with a diameter of 14  $\mu\text{m}$ . In addition, piezoelectric harvesting with ZnO arrays with a zigzag layer has higher efficiency than bulk structures. The results provide useful information for designing and fabricating micro-harvesting devices.

## Keywords

*Piezoelectric; Harvesting; ZnO; Simulation; Electromechanical*

## Introduction

With increasing use of green energy, there is growing demand for higher efficiency energy harvestings [Yasar, 2012]. In general, solar energy, thermal energy, and mechanical vibrations [Philipps, Peharz, Hoheisel,

and Hornung, 2010], [Felix, Ashcon, and Laurent, 2012], [Xianzhi, Yumei, Ping, Yang, and Ming, 2011] can be harvested. Solar cells have been limited in low-light conditions despite their excellent power density. The thermal energy for harvesting is less efficient due to high power consumption. Mechanical vibrations can be converted into electrical energy using electromagnetic, electrostatic and piezoelectric devices. Generally speaking, piezoelectric devices have a high energy conversion for micro-harvesting [Roundy, Leland, Baker, Carleton, and Reilly, 2005] and have great promise for powering electronics and achieving self-powered electronic devices [Chen, Caofeng, Ying, and Zhong, 2012]. The piezoelectric materials such as zirconium titanate (PZT), aluminum nitride (AlN), barium titanate ( $\text{BaTiO}_3$ ), polyvinylidene fluoride (PVDF) and zinc oxide (ZnO) have been used for micro-harvesting [McDonald, Genova, Rosenberg, Keating, Benedixen, and Junru, 2012], [Kumar and Kim, 2012], [Bai, Xu, Gu, Ma, Qin, and Wang, 2012].

In recent years, Al-doped ZnO nanorods have mostly attracted increasing attention due to their conductivity and transparency for applications in optoelectronic devices [Varadhaseshan and Sundar, 2012] [Wu, Wang, and Chen, 2007]. In addition, ZnO nanorods have an extremely stable field emission property [Xue, Li, Yu, Chen, and Yang, 2006] and have been considered for transparent conductive electrodes [Kong, Choi, Cho, Kim, Baek, and Lee, 2010] due to their high transparency, stability and high conductivity. According to reports, the harvesting energy of ZnO nanorods with Al-doped is significantly gets enhanced at peak intensity of c-axis (002) orientation compared to the peak of hexagonal ZnO [Mondal, Kanta, and Mitra, 2008].

In general, the piezoelectric harvesters are bulk [Baù, Ferrari, Tonoli, and Ferrari, 2011] or film [Jing, Miao, Xu, Olfatnia, and Norford, 2010] structures. The

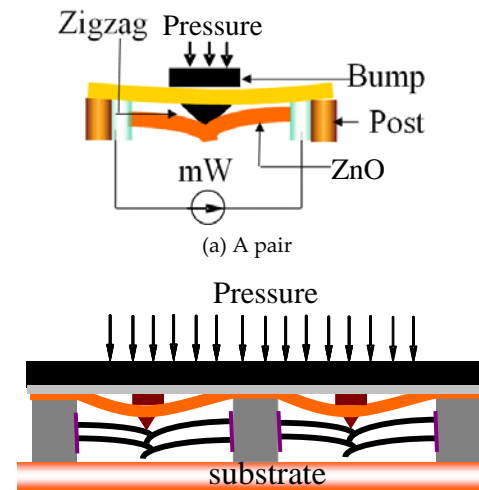
piezoelectric materials exhibit an energy coupling between mechanical deformation and electrical energy when a normal stress is applied. Piezoelectric generators can utilize a cantilever beam, single nanorod or zigzag configuration to harvesting energy [Kanno, Ichida, Adachi, Kotera, and Shibata, 2012]. These structural configurations have a large aspect ratio and critical strain, high flexibility, and sensitivity to small forces. However, few studies have made simulation to determine the piezoelectric harvesting efficiency [Wang, Song, Liu, and Wang, 2007], [Xu, Qin, Xu, Wei, Yang, and Wang, 2010], [Zhu, Yang, Wang, and Wang, 2010].

This study simulates piezoelectric harvesting efficiency of ZnO microstructural arrays with various structural configurations using finite element method (FEM) simulation. The effects of various ZnO structural parameters on a given cross-section areas are simulated, including length, array number and shape of ZnO. In addition, a modal analysis is conducted and the harmonic response of ZnO structures is evaluated to illustrate the excitation frequency at maximum deflection.

## Simulation Setup

### Harvesting Models

Coventor Ware software (Convector, Inc.) was used to simulate the harvesting efficiency of piezoelectric ZnO structures. A pair and an array of piezoelectric structures with a zigzag layer were designed to enhance bending and compression deformation, as shown in FIG. 1(a) and 1(b), respectively. The zigzag structure provides a normal stress and a bending moment to the array of piezoelectric ZnO, which enlarges the electric field due to higher electromechanical coupling. During the simulation, a half symmetry model of the ZnO structures was simulated to reduce memory use and time. The mesh elements of the rectangle and the cylinder were meshed as manhattan and tetrahedrous types, respectively. The mesh size, from 4 to 10  $\mu\text{m}$ , was in accordance with the size of the piezoelectric structures. For the boundary condition, the bottom of the ZnO substrate was considered as rigid and there was no deflection during simulation. A 5  $\mu\text{m}$  thickness rigid cover layer on the top of the piezoelectric structure was used to apply a load. The ZnO structures were assumed to be linear and to have a small deflection under an external load. The mass, damping and stiffness matrices were constant with time during the simulation.



(b) ZnO array rods with zigzag layers that enhance bending and compression deformation

FIG. 1 STRUCTURES USED FOR PIEZOELECTRIC SIMULATION

For modal and harmonic simulations of energy harvesting, rectangular, cylindrical, and 2x2, 4x4, 5x5, and 6x6 arrays of symmetric ZnO models were simulated, as shown in FIG. 2. All structures of the ZnO models had a length of 60  $\mu\text{m}$  and a total cross-section area of about 707  $\mu\text{m}^2$ . The width of the rectangular structure and the diameter of the cylindrical structure were 26.59  $\mu\text{m}$  and 30  $\mu\text{m}$ , respectively. The diameters of the 2x2, 4x4, 5x5, and 6x6 arrays were 15, 7.5, 6 and 5  $\mu\text{m}$ , respectively. The length, width and thickness of the substrate were 50, 50, and 30  $\mu\text{m}$ , respectively, and the thickness of the top layer (not shown) was 5  $\mu\text{m}$ .

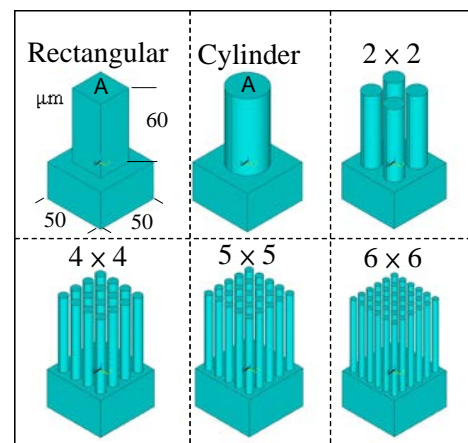


FIG. 2 CHARACTERISTIC SIMULATION OF ZnO MODELS FOR PIEZOELECTRIC HARVESTING FOR A GIVEN TOTAL CROSS-SECTION AREA

### Piezoelectric Harvesting Mechanisms

The mechanisms of piezoelectric harvesting are created using the electromechanical coupling characteristics. The mechanical properties, namely the mechanical stress ( $\sigma$ ) and mechanical strain ( $S$ ), and dielectric

properties, namely the electric field ( $E$ ) and the electric displacement ( $D$ ), of the piezoelectric material were considered. The constitutive equation to describe the piezoelectric properties is based on d-type:

$$\begin{cases} \varepsilon = s^E \sigma + d_t E \\ D = d \sigma + \varepsilon^\sigma E \end{cases} \quad (1)$$

where

$$\begin{aligned} \{\varepsilon\}_{6 \times 1} &= \{\varepsilon_{xx}, \varepsilon_{yy}, \varepsilon_{zz}, 2\varepsilon_{yz}, 2\varepsilon_{xz}, 2\varepsilon_{xy}\}^T, \\ \{\sigma\}_{6 \times 1} &= \{\sigma_{xx}, \sigma_{yy}, \sigma_{zz}, \sigma_{yz}, \sigma_{xz}, \sigma_{xy}\}^T, \\ \{E\}_{3 \times 1} &= \{E_x, E_y, E_z\}, \quad \{D\}_{3 \times 1} = \{D_x, D_y, D_z\} \end{aligned}$$

$s^E$ ,  $d$ , and  $\varepsilon^\sigma$  are the compliance coefficient ( $\text{m}^2/\text{N}$ ), stiffness matrix ( $\text{m/V}$ ) and dielectric constant ( $\text{F/m}$ ), respectively.  $d$  is the transpose of  $d$ . The superscript  $\sigma$  indicates the dielectric constant at a constant mechanical stress. The superscript  $E$  indicates the compliance coefficient at a constant electric field. Assume that the ZnO crystal material is isotropic, orthotropic and polarized along the  $z$  direction. Therefore, the compliance coefficient, stiffness matrix and dielectric constant can be respectively expressed as:

$$[s^E] = \begin{Bmatrix} \varepsilon_{xx} \\ \varepsilon_{yy} \\ \varepsilon_{zz} \\ 2\varepsilon_{yz} \\ 2\varepsilon_{xz} \\ 2\varepsilon_{xy} \end{Bmatrix} = \begin{bmatrix} s_{11}^E & s_{12}^E & s_{13}^E & 0 & 0 & 0 \\ s_{21}^E & s_{22}^E & s_{23}^E & 0 & 0 & 0 \\ s_{31}^E & s_{32}^E & s_{33}^E & 0 & 0 & 0 \\ 0 & 0 & 0 & s_{44}^E & 0 & 0 \\ 0 & 0 & 0 & 0 & s_{55}^E & 0 \\ 0 & 0 & 0 & 0 & 0 & s_{66}^E \end{bmatrix} \quad (2)$$

$$[\varepsilon^\sigma] = \begin{bmatrix} \varepsilon_{11} & 0 & 0 \\ 0 & \varepsilon_{22} & 0 \\ 0 & 0 & \varepsilon_{33} \end{bmatrix} \quad (3)$$

$$[d] = \begin{bmatrix} 0 & 0 & 0 & 0 & d_{15} & 0 \\ 0 & 0 & 0 & d_{24} & 0 & 0 \\ d_{31} & d_{32} & d_{33} & 0 & 0 & 0 \end{bmatrix} \quad (4)$$

Substituting equations (2) to (4) into (1) and representing the result in array form yields:

$$\begin{Bmatrix} \varepsilon_{xx} \\ \varepsilon_{yy} \\ \varepsilon_{zz} \\ 2\varepsilon_{yz} \\ 2\varepsilon_{xz} \\ 2\varepsilon_{xy} \\ D_x \\ D_y \\ D_z \end{Bmatrix} = \begin{bmatrix} s_{11}^E & s_{12}^E & s_{13}^E & 0 & 0 & 0 & 0 & 0 & d_{31} \\ s_{21}^E & s_{22}^E & s_{23}^E & 0 & 0 & 0 & 0 & 0 & d_{32} \\ s_{31}^E & s_{32}^E & s_{33}^E & 0 & 0 & 0 & 0 & 0 & d_{33} \\ 0 & 0 & 0 & s_{44}^E & 0 & 0 & 0 & d_{24} & 0 \\ 0 & 0 & 0 & 0 & s_{55}^E & 0 & d_{15} & 0 & 0 \\ 0 & 0 & 0 & 0 & 0 & s_{66}^E & 0 & 0 & 0 \\ 0 & 0 & 0 & 0 & d_{15} & 0 & \varepsilon_{11} & 0 & 0 \\ 0 & 0 & 0 & d_{24} & 0 & 0 & 0 & \varepsilon_{22} & 0 \\ d_{31} & d_{32} & d_{33} & 0 & 0 & 0 & 0 & 0 & \varepsilon_{33} \end{bmatrix} \begin{Bmatrix} \sigma_{xx} \\ \sigma_{yy} \\ \sigma_{zz} \\ \sigma_{yz} \\ \sigma_{xz} \\ \sigma_{xy} \\ E_x \\ E_y \\ E_z \end{Bmatrix} \quad (5)$$

During the simulation, the compliance coefficients were  $S_{11}=2.097 \times 10^5$ ,  $S_{12}=S_{21}=1.211 \times 10^5$ ,  $S_{22}=2.097 \times 10^5$ ,

$S_{13}=S_{31}=1.051 \times 10^5$ ,  $S_{23}=S_{32}=1.051 \times 10^5$ ,  $S_{33}=2.109 \times 10^5$ ,  $S_{44}=4.430 \times 10^4$  and  $S_{55}=S_{66}=4.240 \times 10^4$  MPa. The stiffness matrices were  $d_{15}=-1.134 \times 10^{-5}$ ,  $d_{26}=-1.134 \times 10^{-5}$ ,  $d_{31}=-5.43 \times 10^{-6}$ ,  $d_{32}=-5.43 \times 10^{-6}$  and  $d_{24}=0$ ,  $d_{33}=1.167 \times 10^{-5}$  pC/(V·μm). The vacuum permittivity, density, and dielectric conductivity were  $\varepsilon_0=8.85 \times 10^{-12}$  C/(V·m), 5.68 g/cm<sup>3</sup> and  $2.5 \times 10^{-1}$  ps/μm, respectively.

## Results and Discussion

The effects of ZnO geometric shape, a modal analysis and a harmonic response evaluation are illustrated in this section.

### Effect of Geometric Shape

Most piezoelectric structures for energy harvesting are designed as rectangular cuboids due to the fabrication process. Rectangular and cylindrical structures with a cross-section area of about 707 μm<sup>2</sup> and a length of 60 μm were simulated at various shear stresses. The width of the rectangular and the diameter of the cylindrical were 26.59 μm and 30 μm, respectively. The length, width and thickness of the substrate were 50, 50 and 30 μm, respectively, and the thickness of top layer was 5 μm. The results show that the harvesting voltages and structural deflections of the cylindrical shape are higher than those of the rectangular cuboid for all shear stresses, as shown in FIG. 3. This is attributed to the fact that the cylindrical shape has a smaller moment of inertia than that of the rectangular cuboid. The moment of inertia means that an object resists rotational moment and torque about an axis.

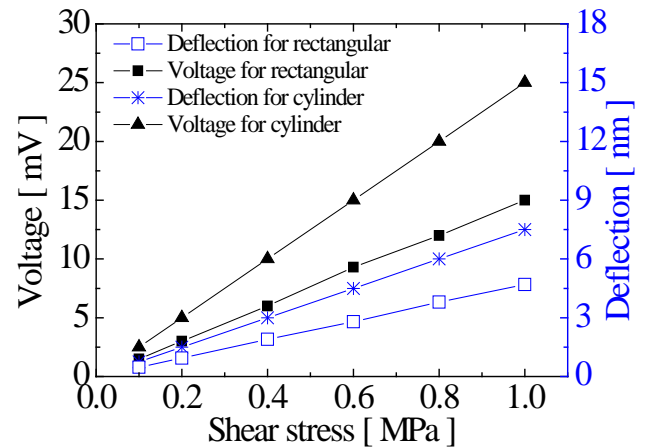


FIG. 3 ENERGY HARVESTING CHARACTERISTICS OF RECTANGULAR AND CYLINDRICAL ZnO STRUCTURES FOR A GIVEN CROSS-SECTION AREA AND LENGTH

FIG. 4 shows voltage versus shear stress for cylindrical structures with various diameters and a constant height of the ZnO cylinder for shear stresses of 1, 0.3, 0.5, 0.7, and 1.0 MPa. A constant height of the ZnO structure is 100 μm and the diameters of the ZnO structure are 20,

40, 60, 80, 100 and 120  $\mu\text{m}$ . The geometric ratios,  $R_h = \phi/h$ , of the diameters,  $\phi$ , and a constant height,  $h$ , are 0.4, 0.6, 0.8, 1.0, and 1.2 for energy harvesting. The harvesting voltage increases with decreasing geometric ratio  $R_h$ . The harvesting voltage versus ZnO diameter for a constant pressure of 1 MPa is shown in the inset of FIG. 4. The harvesting voltage curve becomes almost saturated when the diameter of the piezoelectric ZnO is larger than the height of structure. The curve of the harvesting voltage is similar to negative exponential function.

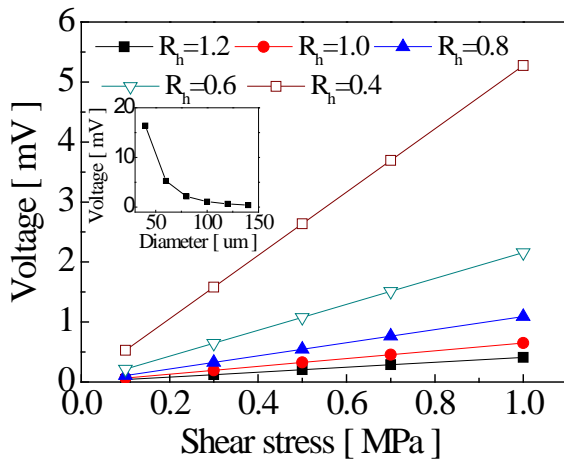


FIG. 4 VOLTAGE VERSUS SHEAR STRESS FOR CYLINDRICAL ZNO STRUCTURES WITH VARIOUS DIAMETERS AND A CONSTANT HEIGHT OF ZNO CYLINDER FOR VARIOUS SHEAR STRESSES

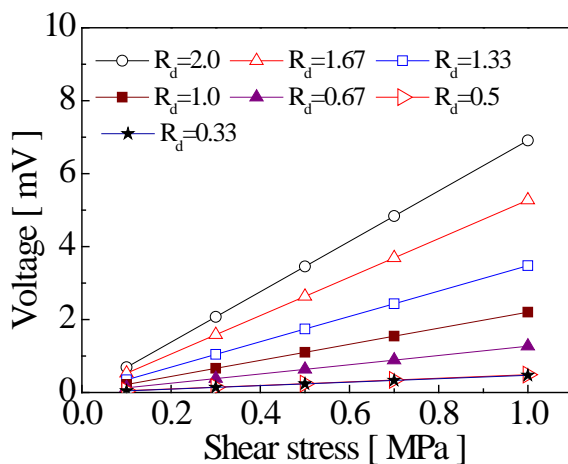


FIG. 5 VOLTAGE VERSUS SHEAR STRESS FOR CYLINDRICAL STRUCTURES WITH VARIOUS HEIGHTS AND A CONSTANT DIAMETER OF ZNO CYLINDER FOR VARIOUS SHEAR STRESSES

FIG. 5 shows voltage versus shear stress for cylindrical structures with various heights and a constant diameter for shear stresses of 1, 0.3, 0.5, 0.7 and 1.0 MPa. The ratios  $R_d$  is defined as the heights ( $h$ ) of ZnO cylinder and a constant diameter ( $\phi$ ) of ZnO cylinder. The ratios,  $R_d = h/\phi$ , of ZnO cylinder for energy harvesting simulation are 2, 1.67, 1.0, 0.67, 0.5 and 0.33. The diameter of the ZnO structure is 60  $\mu\text{m}$  and the heights of the ZnO structure are 20, 30, 40, 60, 100 and

120  $\mu\text{m}$ . The results show that the harvesting voltages of the ZnO structure increase with increasing geometric ratio  $R_d$ . The harvesting voltages for  $R_d$  equal 2, 1.67, 1.0, 0.67, 0.5 and 0.33 at a shear stress of 1 MPa are 6.9, 5.23, 2.2, 1.27, 0.49 and 0.48 mV, respectively. The conversion efficiencies of  $R_d = 0.33, 0.5$  and  $0.67$  decreased 78.2, 77.7 and 42.3 %, respectively, compared to the geometric effect of  $R_d = 1$ . However, the conversion efficiencies of  $R_d = 1.67$  and  $2.0$  increased 137.7 and 213.6%, respectively, also compared to the geometric effect of  $R_d = 1$ . The harvesting voltage trend of the ZnO becomes almost saturated when the  $R_d$  ratio is less than 0.5. It can be predicted that there has small electric dipole moment when the  $R_d$  is less than 0.5.

### Modal and Harmonic Analysis

In general, the harvesting mechanism of a piezoelectric structure is produced from structural resonances due to vibrations at the excitation frequency. A modal analysis can be used to determine the natural mode shapes and the resonant frequencies of the ZnO structures for optimal energy harvesting during free vibration. FIG. 6 shows the ZnO modal analysis results of a rectangular, a cylindrical, and 2x2, 4x4, 5x5, and 6x6 array structures with the same total cross-section areas. Simulation results show that the rectangular ZnO structure has a lower resonant frequency than that of the cylindrical structure at different modal types. It is supposed that a rectangular has larger second moment of area than a cylinder. A ZnO structure with fewer arrays has a higher resonant frequency. Therefore, a structure with a low resonant frequency is more efficient for energy harvesting due to a less amount of driving energy. The energy harvesting for microstructures at high-frequency MHz range is not suitable for the use of array structures.

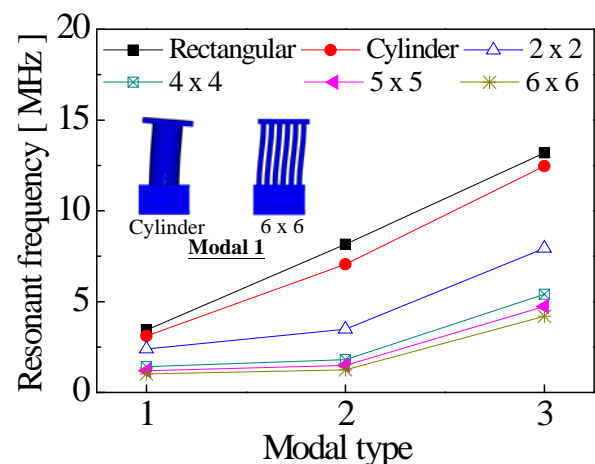


FIG. 6 ZNO MODAL ANALYSIS RESULTS FOR A RECTANGULAR, A CYLINDRICAL, AND 2x2, 4x4, 5x5 AND 6x6 ARRAY STRUCTURES FOR A GIVEN TOTAL CROSS-SECTION AREA

The time-dependent equations of ZnO motion undergoing steady-state vibration were analyzed. All loads and deflections sinusoidally vary at a given frequency. The harmonic analyses can be used to obtain the deflection amplitudes of ZnO vibration at given points in the structures as a function of forcing frequency. FIG. 7 shows the harmonic deflections of various ZnO models for various harmonic forces at a constant resonant frequency. The ZnO model with a 6×6 array had the highest deflection for a given harmonic force. Energy harvesting efficiency of ZnO array increases with the increasing deflection. The deflections of a rectangular, a cylindrical, and 2×2, 4×4, 5×5 and 6×6 array structures at a harmonic force of 500  $\mu\text{N}$  were 0.708, 0.943, 4.215, 6.759, 9.786 and 14.748  $\mu\text{m}$ , respectively. Therefore, ZnO structures for energy harvesting should be designed as an array of cylinders.

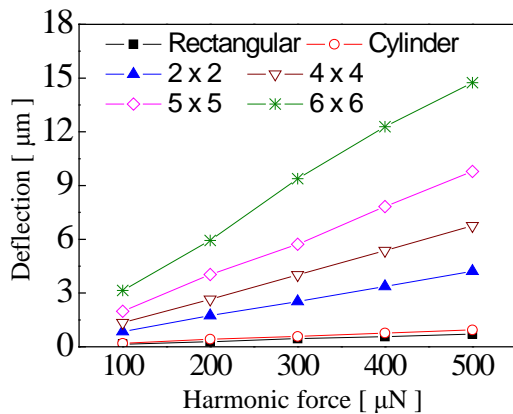


FIG. 7 HARMONIC DEFLECTIONS OF ZnO MODELS FOR A GIVEN CROSS-SECTION AREA AND VARIOUS HARMONIC FORCES AT A CONSTANT FREQUENCY

### Array Analysis

The energy harvesting of single bulk and array structures with a given cross-section area and a height of 100  $\mu\text{m}$  were investigated under various shear stresses. The diameter and the height of the single bulk were 60 and 100  $\mu\text{m}$ , respectively. The diameters of ZnO with 6, 11, 19, 22 and 33 arrays were 30, 24, 19, 16 and 14  $\mu\text{m}$ , respectively. The harvesting voltages of a single bulk are smaller than those of the arrays, as shown in FIG. 8. In addition, the harvesting voltage of ZnO array increased with increasing number of arrays. The voltages for 1, 6, 11, 19 and 22 arrays are 0.543, 1.05, 1.56, 2.42 and 3.46 mV, respectively. The conversion efficiencies of 6, 11, 19 and 22 arrays increase 93.4, 187.3, 345.6 and 537.2 %, respectively, compared to the single bulk output powers. The harvesting energy of ZnO decreased when the number of arrays was over 33. The structure rigidity increases with increasing number of arrays.

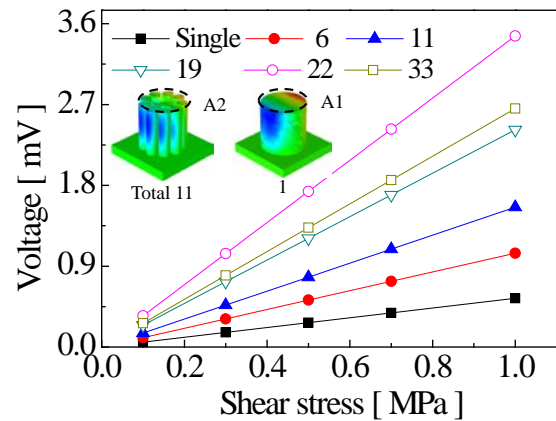


FIG. 8 PIEZOELECTRIC HARVESTING RESULTS FOR A SINGLE STRUCTURE AND 6, 11, 19, 22, AND 33 ARRAYS

### Conclusion

The energy harvesting characteristics of zinc oxide for microharvesters were investigated. The harvesting voltage curve becomes almost saturated when the diameter of the piezoelectric ZnO is larger than the height of the structure (about 100  $\mu\text{m}$ ). A rectangular ZnO structure has a lower resonant frequency than a cylindrical structure for a given cross-section area at different modal types. The harvesting voltage of ZnO increased with increasing number of arrays. However, the harvesting energy of ZnO decreased when the number of arrays was over 33. The results show that ZnO can be applied to electromechanical nanogenerators.

### ACKNOWLEDGEMENTS

This work was supported by the National Science Council of Taiwan (under grant NSC 101-2221-E-150-013 and NSC 101-2221-E-150-014).

### REFERENCES

- Bai, S., Xu, Qi, Gu, L., Ma, F., Qin, Y., Wang, Z.L., "Single Crystalline Lead Zirconate Titanate (PZT) Nano/Micro-wire Based Self-powered UV Sensor", *Nano Energy*, Vol. 1(6), 2012, PP. 789-795.
- Baù, M., Ferrari, M., Tonoli, E., Ferrari, V., "Sensors and energy harvesters based on piezoelectric thick films", *Procedia Engineering*, Vol. 25, 2011, PP. 737-744.
- Chen, X., Caofeng, P., Ying, L., Zhong, L.W., "Hybrid Cells for Simultaneously Harvesting Multi-type Energies for Self-Powered Micro/Nanosystems", *Nano Energy*, Vol. 1(1), 2012, PP. 259-272.
- Felix, Y.L., Ashcon, N., Laurent, P., "Pyroelectric Waste Heat Energy Harvesting Using Heat Conduction", *Applied*



- Thermal Engineering, Vol. 37(1),2012,PP. 30-37.
- Jing, X.M., Miao, J.M., Xu, T., Olfatnia, M., Norford, L.V., "Vibration Characteristics of Micromachined Piezoelectric Diaphragms with a Standing Beam Subjected to Airflow", *Sensors and Actuators A: Physical*, Vol. 164(1-2), 2010, PP. 22-27.
- Kanno, I., Ichida, T., Adachi, K., Kotera, H., Shibata, K., "Tomoyoshi Mishima Power-generation Performance of Lead-free (K,Na) NbO<sub>3</sub> Piezoelectric Thin-film Energy Harvesters", *Sensors and Actuators A: Physical*, Vol. 179, 2012, PP. 132-136.
- Kong, B.H., Choi, M.K., Cho, H.K., Kim, J.H., Baek, S., Lee, J.H., "Conformal Coating of Conductive ZnO: Al Films as Transparent Electrodes on High Aspect Ratio Si Microrods", *Electrochem Solid-State Lett.*, Vol. 13(1), 2010, PP. K12-K14.
- Kumar, B., Kim, S.W., "Energy Harvesting Based on Semiconducting Piezoelectric ZnO Nanostructures Review Article", *Nano Energy*, Vol.1(3), 2012,PP. 342-355.
- McDonald, T.G., Genova, V., Rosenberg, S., Keating, J., Benedixen, C., Junru, W., "Experimental and Theoretical Studies on MEMS Piezoelectric Vibrational Energy Harvesters with Mass Loading", *Sensors and Actuators A: Physical*, Vol. 178(1), 2012, PP. 76-87.
- Mondal, S., Kanta, K.P., Mitra, P., "Preparation of Al-doped ZnO (AZO) Thin Film by SILAR", *Journal of Physical Sciences*, Vol. 12, 2008, PP. 221-229.
- Philipps, S.P., Peharz, G., Hoheisel, R., Hornung, T., et al. "Energy Harvesting Efficiency of III-V Triple-junction Concentrator Solar Cells under Realistic Spectral Conditions", *Solar Energy Materials and Solar Cells*, Vol. 94(5), 2010, PP. 869-877.
- Roundy, S., Leland, E.S., Baker J., Carleton, E., Reilly, E., Lai, E., Otis, B., Rabaey, J.M., Wright, P.K., Sundararajan, V., "Improving Power Output for Vibration-based Energy Scavengers", *IEEE Pervasive Compt.*, Vol. 4(1),2005, PP. 28-36.
- Varadhaseshan, R., Sundar, S. M., "Existence of Ferromagnetism and Structural Characterization of Nickel Doped ZnO Nanocrystals", *Applied Surface Science*, Vol. 258(18), 2012, PP. 7161-7165.
- Wang, X., Song, J., Liu, J., Wang, Z.L., "Direct Current Nanogenerator Driven by Ultrasonic Wave", *Science*, Vol. 316(1), 2007, PP. 102-105.
- Wu, K.Y., Wang, C.C., Chen, D.H., "Preparation and Conductivity Enhancement of Al-doped Zinc Oxide Thin Films Containing Trace Ag Nanoparticles by the Sol-Gel Process", *Nanotechnology*, Vol. 18 (1), 2007, PP. 305604.
- Xianzhi, D., Yumei, W., Ping, L., Yang, J., Ming, L., "Energy Harvesting from Mechanical Vibrations Using Multiple Magnetostrictive/Piezoelectric Composite Transducers", *Sensors and Actuators A: Physical*, Vol. 166(1), 2011, PP. 94-101.
- Xu, S., Qin, Y., Xu, C., Wei, Y., Yang, R., Wang, Z.L., "Self-powered Nanowire Devices", *Nature Nanotechnology*, Vol. 5(1), 2010, PP. 366-373.
- Xue, X.Y., Li, L.M., Yu, H.C., Chen, Y.J., Yang, Y.G., "Extremely Stable Field Emission from AlZnO Nanowire Arrays", *Appl. Phys. Lett.*, Vol. 89, 2006, PP. 043118-1-3.
- Yasar, D., "Green Energy and Technology", *Energy Conservation*, Vol. 1, 2012, PP. 343-395.
- Zhu, G., Yang, R., Wang, S., Wang, Z.L., "Flexible High-output Nanogenerator Based on Lateral ZnO Nanowire Array", *Nano Lett.*, Vol. 10(8), 2010, PP. 3151-5.